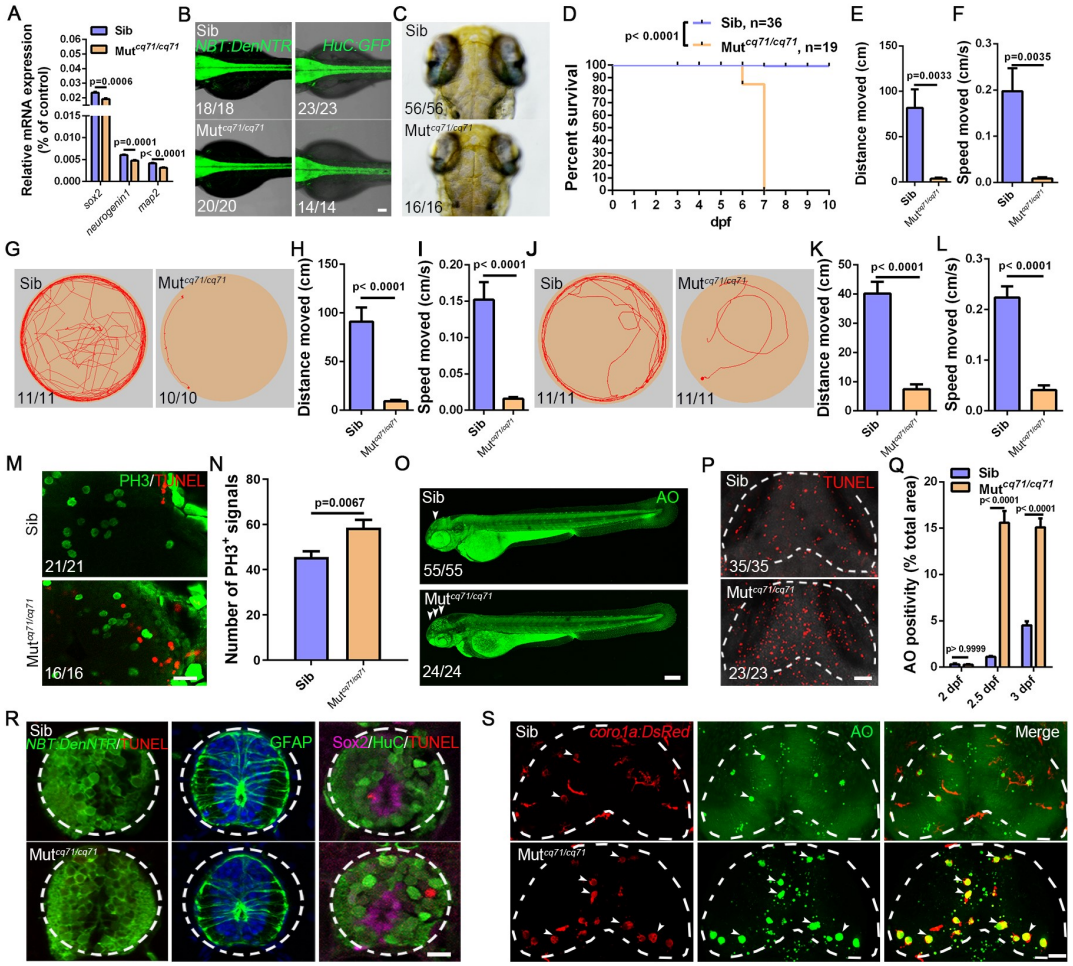

Fig. S1. Compromised neurogenesis in Mut$^{cq71/cq71}$ mutants.

A. The relative expression of *sox2*, *neurogenin1* and *map2* in the head of 2.5 dpf siblings and Mut$^{cq71/cq71}$ mutants by qRT-PCR (Mean ± SEM; *sox2:* sibling, 0.0235 ± 0.0006 n=6, Mut$^{cq71/cq71}$, 0.0192 ± 0.0006 n=6; *neurogenin1:* sibling, 0.0060 ± 0.0001 n=6, Mut$^{cq71/cq71}$, 0.0047 ± 0.0002 n=6; *map2:* sibling, 0.0042 ± 0.0001 n=6, Mut$^{cq71/cq71}$, 0.0031 ± 0.0001 n=6; two independent clutches; unpaired t-test).

B. The fluorescent images of NBT-DenNTR^{+} and HuC-GFP^{+} signals in the corresponding reporter larvae.

C. Bright-field images of the head morphologies.

D. Kaplan–Meier survival curve (log-rank/Mantel–Cox statistic).

E-F. The statistical data of overall distance (E) (Mean ± SEM; sibling, 81.74 ± 20.34 n=6; Mut$^{cq71/cq71}$, 3.55 ± 1.22 n=6; two independent clutches; unpaired t-test) and speed (F) (Mean ± SEM; sibling, 0.20 ± 0.05 n=6; Mut$^{cq71/cq71}$, 0.01 ± 0.002 n=6; two independent clutches; unpaired t-test) of the spontaneous swimming behaviors.

G-I. Representative movement traces after needle touch (G) and the statistical data of overall distance (H) (Mean ± SEM; sibling, 40.18 ± 3.97 n=11; Mut$^{cq71/cq71}$, 7.42 ± 1.68 n=11; two independent clutches; unpaired t-test) and speed (I) (Mean ± SEM: sibling, 0.22 ± 0.02 n=11; Mut$^{cq71/cq71}$, 0.041 ± 0.01 n=11; two independent clutches; unpaired t-test) **J-L.** Representative movement traces after light dark stimulation (J) and the statistical data of overall distance (K) (Mean ± SEM; sibling, 91.06 ± 14.58 n=11; Mut$^{cq71/cq71}$, 9.38 ± 1.39 n=10; two independent clutches; unpaired t-test) and speed (L) (Mean ± SEM; sibling, 0.15 ± 0.02 n=11; Mut$^{cq71/cq71}$, 0.02 ± 0.002 n=10; two independent clutches; unpaired t-test).

M-N. The fluorescent images (M) and quantification (N) of PH3$^+$ (green) and TUNEL$^+$ (red) signals in the midbrains (Mean ± SEM; sibling, 45.64 ± 2.44 n=11; Mut$^{cq71/cq71}$, 58.55 ± 3.50 n=11; two independent clutches; unpaired t-test).

O. The fluorescent images of AO$^+$ signals in the whole embryos.

P. The immunofluorescent images of TUNEL in the midbrains (white dash lines).

Q. The quantification of AO$^+$ signals in the midbrains (Mean ± SEM; 2 dpf: sibling, 0.31 ± 0.10 n=13, Mut$^{cq71/cq71}$, 0.26 ± 0.06 n=15; 2.5 dpf: sibling, 1.13 ± 0.09 n=15, Mut$^{cq71/cq71}$, 15.60 ± 1.25 n=15; 3 dpf: sibling, 4.52 ± 0.43 n=17, Mut$^{cq71/cq71}$, 15.10 ± 0.98 n=18; two independent clutches; unpaired t-test).

R. The immunofluorescent images of NBT-DenNTR/TUNEL, GFAP, Sox2/HuC/TUNEL on the transverse sections of the spinal cord (white dash lines).

S. The fluorescent images of AO$^+$ and coro1a-DsRed$^+$ signals in the midbrains (white dash lines). The white arrowheads indicate the large AO$^+$ foci aggregated in the coro1a-DsRed$^+$ cells.

Scale bars in B, M, P, R, S, 20μm; O, 200 μm.

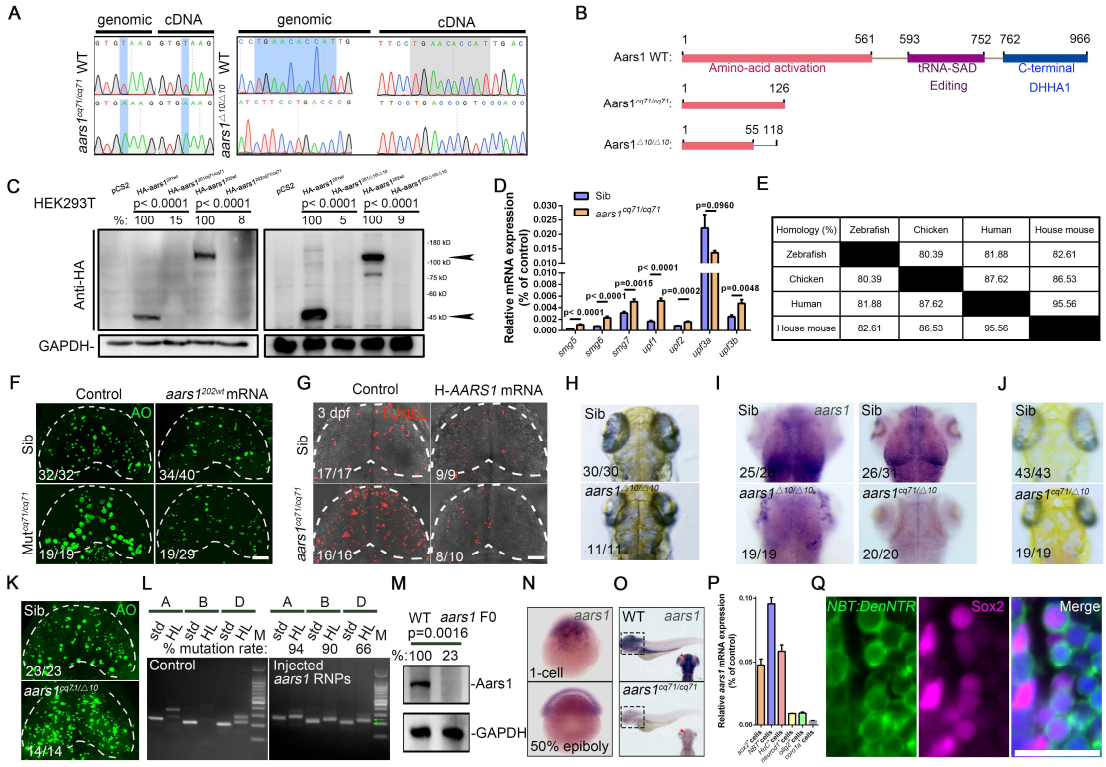

Fig. S2. *aars1* is evolutionarily conserved in regulating neural survival.

A. Sequencing data of genomic and cDNA of WT, *aars1*$^{cq71/cq71}$ and *aars1*$^{\triangle 10/\triangle 10}$ mutant embryos. The shaded areas show the mutation sites.

B. Schematic diagrams of Aars1 protein domains of WT (top), *aars1*$^{cq71/cq71}$ (middle) and *aars1*$^{\triangle 10/\triangle 10}$ mutants (bottom).

C. Western blot of HA-tagged WT and mutant forms of aars1^{201} and aars1^{202}. The GAPDH is used as a control. The protein levels of HA-aars1$^{201cq71/cq71}$ and HA-aars1$^{201\triangle 10/\triangle 10}$ reduced by 85% (P<0.0001) and 95% (P<0.0001), respectively, compared to that in aars1^{201wt}. The protein levels of HA-aars1$^{202cq71/cq71}$ and HA-aars1$^{202\triangle 10/\triangle 10}$ reduced by 92% (P<0.0001) and 91% (P<0.0001), respectively, compared to that in aars1^{202wt}.

D. The expression of NMD-related gene in the head by qRT-PCR (Mean ± SEM; n=8 in each group; two independent clutches; unpaired t-test).

E. AARS1 homology comparing among zebrafish, chicken, human and house mouse.

F. The fluorescent images AO^{+} signals in the midbrains (white dash lines) of siblings and *aars1*$^{cq71/cq71}$ mutants after injecting *aars1*^{202wt} mRNA.

G. The immunofluorescent images of TUNEL in the midbrains (white dash lines) of siblings and *aars1*$^{cq71/cq71}$ mutants after injecting *H-AARS1* mRNA.

H. Bright-field images of *aars1*$^{\triangle 10/\triangle 10}$ and sibling heads.

I. WISH of *aars1* in the brains of *aars1*$^{\triangle 10/\triangle 10}$ (left), *aars1*$^{cq71/\triangle 10}$ (right) and their siblings.

J. Bright-field images of *aars1*$^{cq71/\triangle 10}$ and sibling heads.

K. The fluorescent images of AO^+ signals in the midbrains (white dash lines).

L. RNP target loci (A, B, D) of *aars1* amplified by the sequencing PCR primers (std, standard) or by a headloop primer (HL). Green arrows indicate the ~200-bp ladder band. The mutated efficiency: Guide A , 94%; Guide B, 90%; Guide D, 66%.

M. Western blot of Aars1. The protein levels of Aars1 reduced by 77% in the *aars1* F0 compared to that in the WT control (P=0.0016).

N-O. WISH of *aars1* at different stages.

P. qRT-PCR of *aars1* transcripts in the *sox2*$^+$, *NBT*$^+$, *HuC*$^+$, *neurod1*$^+$, *olig2*$^+$ and *coro1a*$^+$ cells (Mean ± SEM; *sox2*$^+$ 0.048 ± 0.005 n=8; *NBT*$^+$ 0.096 ± 0.005 n=8; *HuC*$^+$ 0.059 ± 0.005 n=8; *neurod1*$^+$ 0.009 ± 0.0001 n=8; *olig2*$^+$ 0.009 ± 0.001 n=8; *coro1a*$^+$ 0.003 ± 0.0001 n=8; two independent clutches).

Q. The immunofluorescent images of Sox2 and *NBT:DenNTR* in the brains after double staining. Scale bars in F, G, K, P, 20 μm.

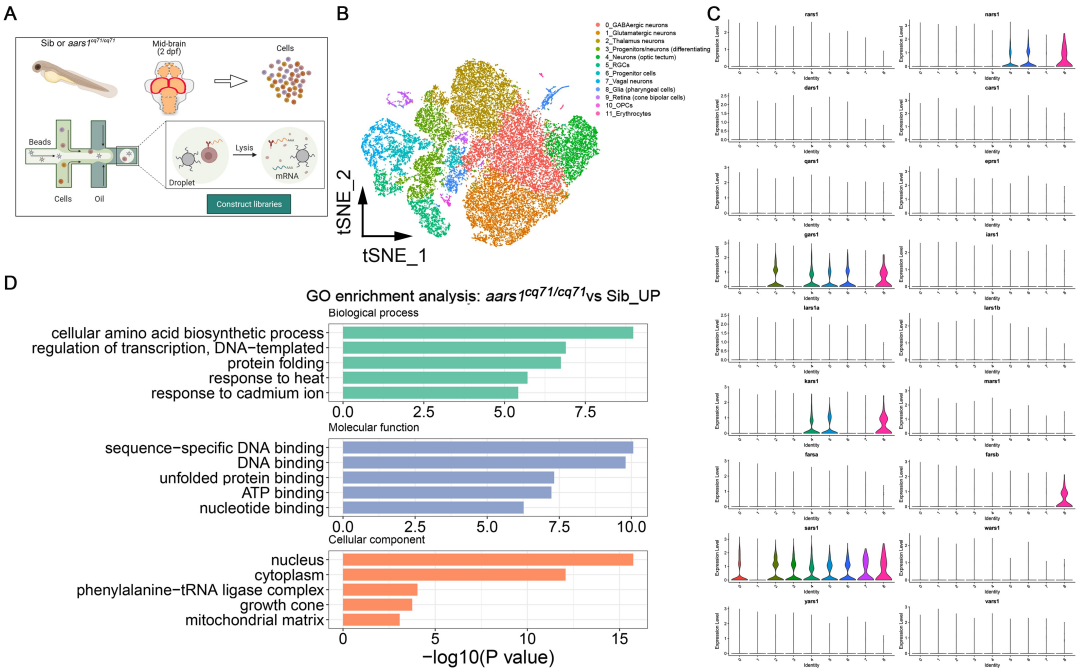

Fig. S3. GO analysis and differential expression of aminoacyl-tRNA synthetases in neuronal progenitors.

A. Schematic workflow of scRNA-seq.

B. Graph-based clustering of collected cells from siblings and *aars1*$^{cq71/cq71}$ mutants.

C. Violin plots (VLN) showing the transcript intensities of various aminoacyl-transfer RNA (tRNA) synthetases in nine neural cell clusters.

D. GO enrichment analysis of the five most affected signaling pathways in biological process, molecular function and cellular component in the *aars1*$^{cq71/cq71}$ PCs.

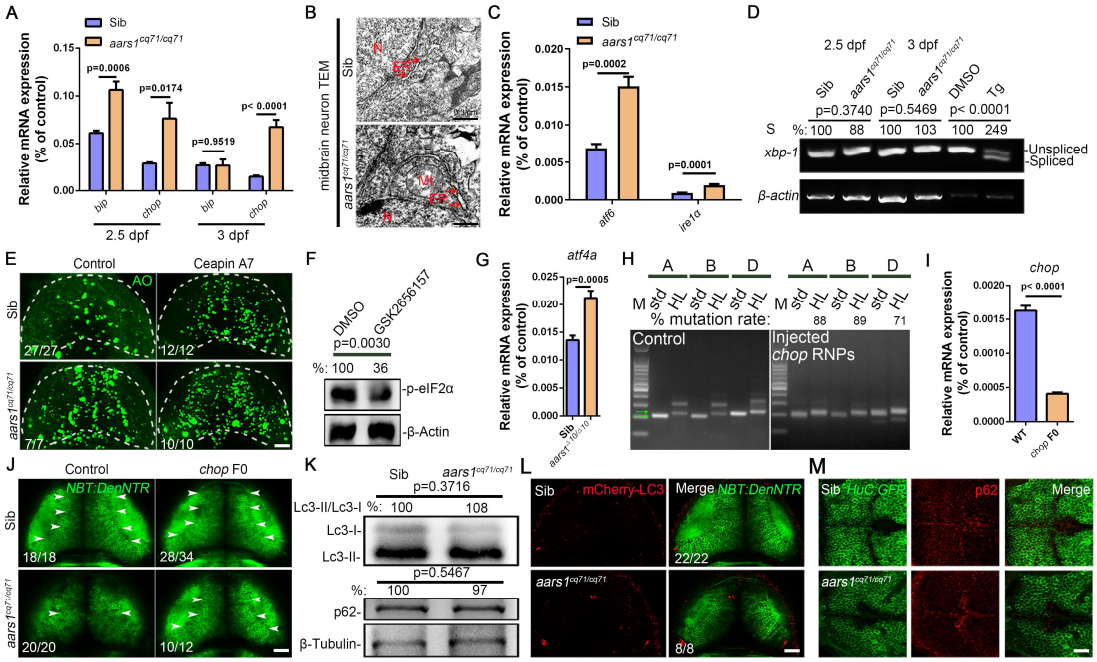

Fig. S4. The Perk signaling but not autophagy pathway is activated in *aars1*$^{cq71/cq71}$ mutants.

A. The transcript amounts of *bip* and *chop* in the head by qRT-PCR (Mean ± SEM; 2.5 dpf: sibling *bip* 0.0611 ± 0.0026 n=6, *aars1*$^{cq71/cq71}$ *bip* 0.1064 ± 0.0089 n=6, sibling *chop* 0.0299 ± 0.0013 n=6, *aars1*$^{cq71/cq71}$ *chop* 0.0764 ± 0.0166 n=6; 3 dpf: sibling *bip* 0.0271 ± 0.0023 n=6, *aars1*$^{cq71/cq71}$ *bip* 0.0267 ± 0.0065 n=6, *chop* sibling 0.0149 ± 0.0013 n=6, *aars1*$^{cq71/cq71}$ *chop* 0.0676 ± 0.0075 n=6; two independent clutches; unpaired t-test).

B. Endoplasmic reticulum structure in siblings and *aars1*$^{cq71/cq71}$ at 3 dpf by transmission electron microscope. N: nucleus; ER: endoplasmic reticulum (red arrows); Mt: mitochondria.

C. The transcript amounts of *atf6* and *ire1α* in the head by qRT-PCR (Mean ± SEM; *atf6:* sibling 0.0069 ± 0.0006 n=6, *aars1*$^{cq71/cq71}$ 0.0151 ± 0.0013 n=6; *ire1α:* sibling 0.0009 ± 0.0001 n=6, *aars1*$^{cq71/cq71}$ 0.0020 ± 0.0002 n=6; two independent clutches; unpaired t-test).

D. RT-PCR of *xbp-1* splicing in siblings and *aars1*$^{cq71/cq71}$. Treating 24 hpf WT embryos with Tg for 1 h is used as a positive control. S, spliced *xbp-1*. The spliced-*xbp-1* levels are increased by 149% (P<0.0001) in the Tg group relative to the controls.

E. The fluorescent images of AO^{+} signals in the midbrains (white dash lines) of siblings and *aars1*$^{cq71/cq71}$ mutants with or without Ceapin A7 treatment.

F. Western blotting of p-eIF2α. The p-eIF2α protein levels are reduced by 64% in the GSK2656157 group compared to the DMSO control (P=0.0030).

G. The transcript levels of *atf4a* in the head by qRT-PCR (Mean ± SEM; sibling, 0.0136 ± 0.0008 n=6; *aars1*$^{cq71/cq71}$, 0.0212 ± 0.0013 n=6; two independent clutches; unpaired t-test).

H. RNP target loci (A, B, D) of *chop* amplified by the sequencing PCR primers (std, standard) or by a headloop primer (HL). Green arrows indicate the ~200-bp ladder band. The mutated efficiency: Guide A , 88%; Guide B, 89%; Guide D, 71%.

I. The transcript amounts of *chop* by qRT-PCR (Mean ± SEM; WT, 0.0016 ± 0.0001 n=12; *chop* F0, 0.0004 ± 0.0001 n=12; two independent clutches; unpaired t-test).

J. The fluorescent images of *NBT:DenNTR* in the brains of siblings and *aars1*$^{cq71/cq71}$ mutants after injecting *chop* RNPs. The white arrowheads indicate the NBT-DenNTR^{+} signals.

K. Western blot of Lc3-II/Lc3-I and p62. The β-tubulin is used as a control.

L. The immunofluorescent staining images of mCherry-LC3 and *NBT:DenNTR* in the brains of siblings and *aars1*$^{cq71/cq71}$ mutants.

M. The immunofluorescent staining images of *HuC:GFP* and P62 on the transverse sections of the midbrains.

Scale bars in E, H, J, K, 20 μm; B, 0.3 μm.

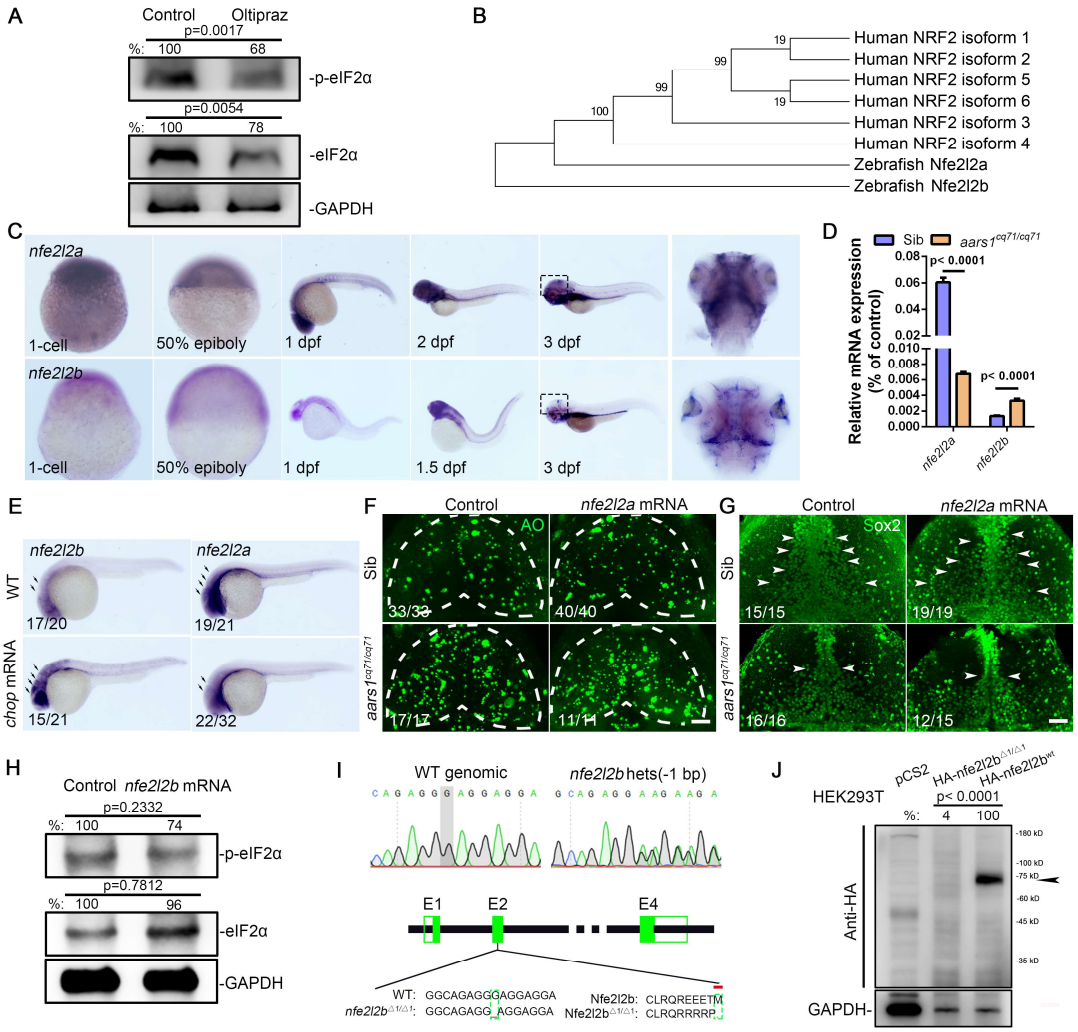

Fig. S5. *nfe2l2b,* but not *nfe2l2a,* contributes to the regulation of neural survival in *aars1*$^{cq71/cq71}$ mutants.

A. Western blot of p-eIF2α and eIF2α in the embryos treating with Oltipraz. The GAPDH is used as a control. The protein levels of p-eIF2α and eIF2α are reduced by 32% (P=0.0017) and 22% (P=0.0054) in the *aars1*$^{cq71/cq71}$ mutants compared to the control.

B. A phylogenetic tree of the full-length Nrf2 amino acid sequences constructed by the neighbor-joining method.

C. WISH of *nfe2l2a* (top) and *nfe2l2b* (bottom) at different stages.

D. The transcript amounts of *nfe2l2a* and *nfe2l2b* in the head by qRT-PCR (Mean ± SEM; *nfe2l2a:* sibling 0.0605 ± 0.0035 n=6, *aars1*$^{cq71/cq71}$ 0.0067 ± 0.0002 n=6; *nfe2l2b*: sibling 0.0014 ± 0.0001 n=6, *aars1*$^{cq71/cq71}$ 0.0033 ± 0.0002 n=6; two independent clutches; unpaired t-test).

E. WISH of *nfe2l2b* (left) and *nfe2l2a* (right) in the embryos after injecting *chop* mRNA. The arrowheads indicate the signals.

F-G. The fluorescent images of AO^+ (F) and Sox2+ (G) signals in the midbrains (white dash lines) after injecting *nfe2l2a* mRNA. White arrowheads indicate the $Sox2^+$ signals.

H. Western blot of p-eIF2α and eIF2α in the embryos. The GAPDH is used as a control. The p-eIF2α protein levels are reduced by 26% (P=0.2332) in the *nfe2l2b* mRNA group. **I.** The genomic sequencing of targeted regions in WT and *nfe2l2b*$^{\triangle 1/+}$ (upper). The shaded area highlights the mutation site. Deletion of 1 bp leads to the early termination of Nfe2l2b translation in *nfe2l2b*$^{\triangle 1/\triangle 1}$ (bottom).

J. Western blot of HA. The GAPDH is used as a control. The protein levels of HA-nfe2l2b$^{\triangle 1/\triangle 1}$ are reduced by 96% compared to HA-nfe2l2b^{wt} (P<0.0001).

Scale bar in F, G, 20 μm.

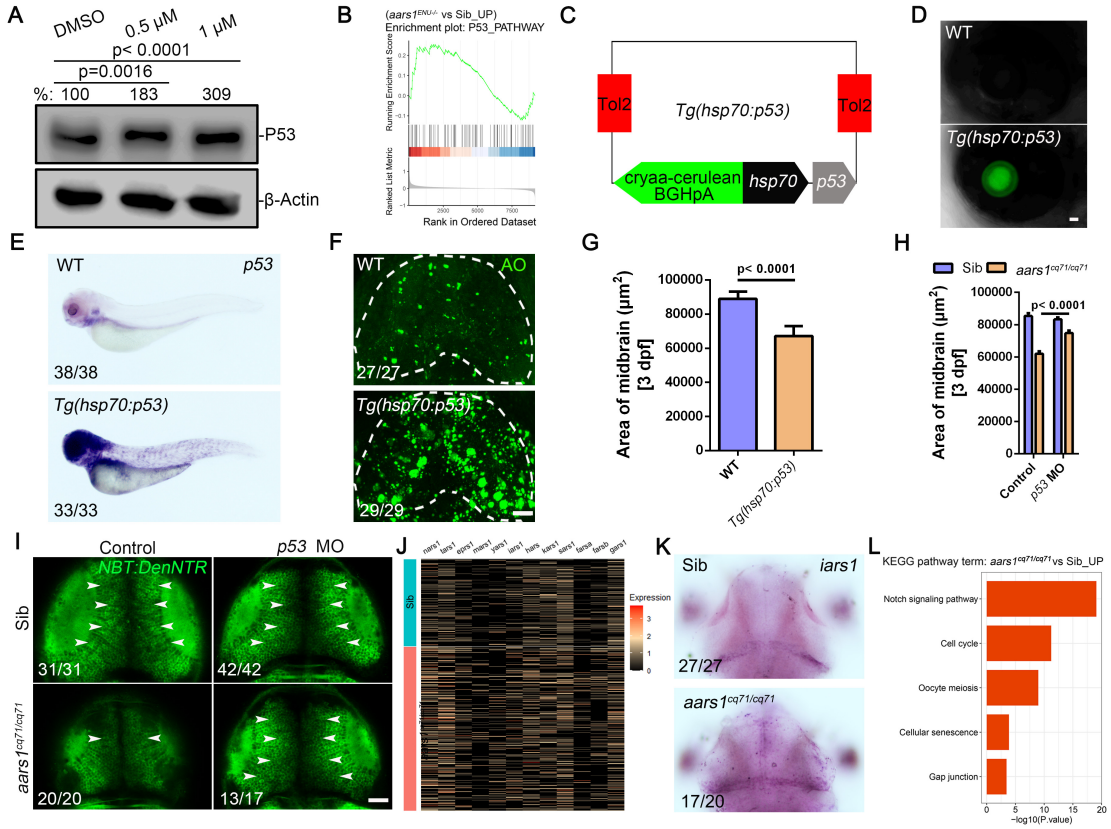

Fig. S6. Over activation of P53 promotes neural apoptosis

A. Western blot of P53 in 293T cells treating with 0.5 μM or 1 μM Tg. The β-Actin is used as a control. The protein levels of P53 are increased by 83% (P=0.0016) and 209% (P<0.0001) in the 0.5 μM and 1 μM Tg groups, respectively, compared to that in the control.

B. GSEA enrichment of the up-regulated P53 pathway in cluster 4 of *aars1*$^{cq71/cq71}$ mutants.

C. The construction of *pT2AL-hsp70:p53; cryaa:cerulean* vector.

D. Representative fluorescent images of the lens in *Tg(hsp70:p53)*.

E. WISH of *p53* in WT and *Tg(hsp70:p53)* embryos after heat shock.

F. The fluorescent images of AO^{+} signals in the midbrains (white dash lines) of WT and *Tg(hsp70:p53)* after heat shock.

G. Quantification of the midbrain size of WT and *Tg(hsp70:p53)* after heat shock (Mean ± SEM; WT, 88845 ± 1656 n=7; *Tg(hsp70:p53),* 67185 ± 2194 n=7; two independent clutches; unpaired t-test).

H. Quantification of midbrain size (Mean ± SEM; control: sibling, 85374.49 ± 1833.10 n=9,

aars1$^{cq71/cq71}$, 61988.01 ± 1592.02 n=9; *p53* MO: sibling, 83299.14 ± 1168.72 n=18, *aars1*$^{cq71/cq71}$, 74753.43 ± 1586.78 n=12; two independent clutches; two-way ANOVA).

I. The fluorescent images of *NBT:DenNTR* in the brains of siblings and *aars1*$^{cq71/cq71}$ mutants after injecting *p53* MO. The arrowheads indicate the signals.

J. Heatmap of the up-regulated aminoacyl-transfer RNA (tRNA) synthetase genes in 2 dpf *aars1*$^{cq71/cq71}$ PCs.

K. WISH of *iars1* in siblings and *aars1*$^{cq71/cq71}$ mutants.

L. KEGG pathway term of the five up-regulated pathways in *aars1*$^{cq71/cq71}$ PCs.

Scale bar in D, F, I, 20 μm.

Table S1. Primers used

Click here to download Table S1

Table S2. Key resources

Click here to download Table S2

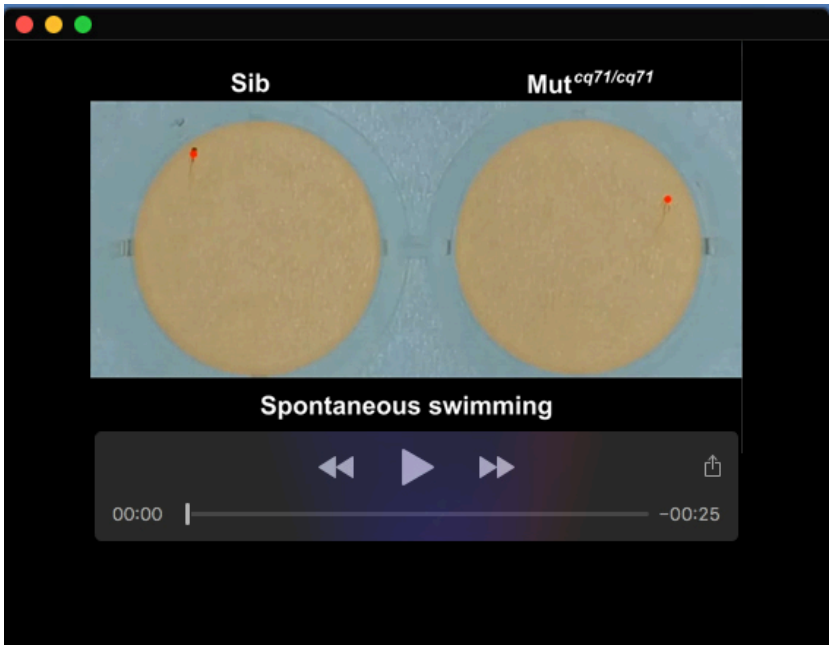

Movie 1. Spontaneous swimming behavior of sibling and Mut$^{cq71/cq71}$ mutant embryos. Related to Figure 1. Five minutes track records of the swimming behaviors on 3 dpf embryos after a 5-minute adaptation. The yellow circle area represents the imaging field. The red line represents the swimming track. This video presented the behavioral recording in Figure 1B.

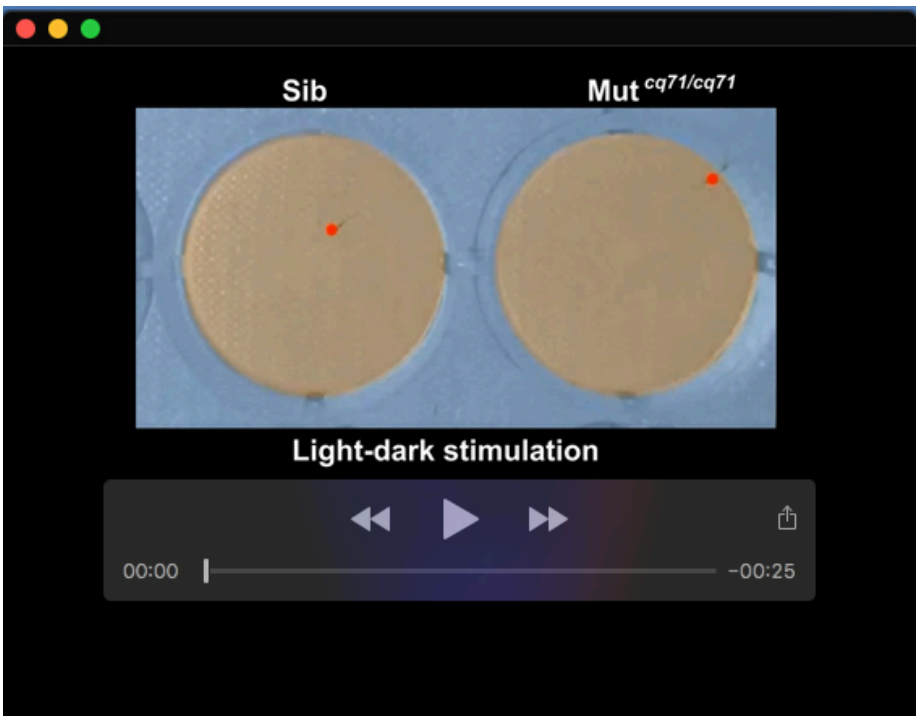

Movie 2. The sibling and Mut$^{cq71/cq71}$ mutant reactions on the light-dark stimulation. Related to Figure S1. Ten minutes track records of the swimming behaviors on 5 dpf larvae after a 5-minute darkness stimulation. The yellow circle area represents the imaging field. The red line represents the swimming track. This video presented the behavioral recording in Supplemental 1G.

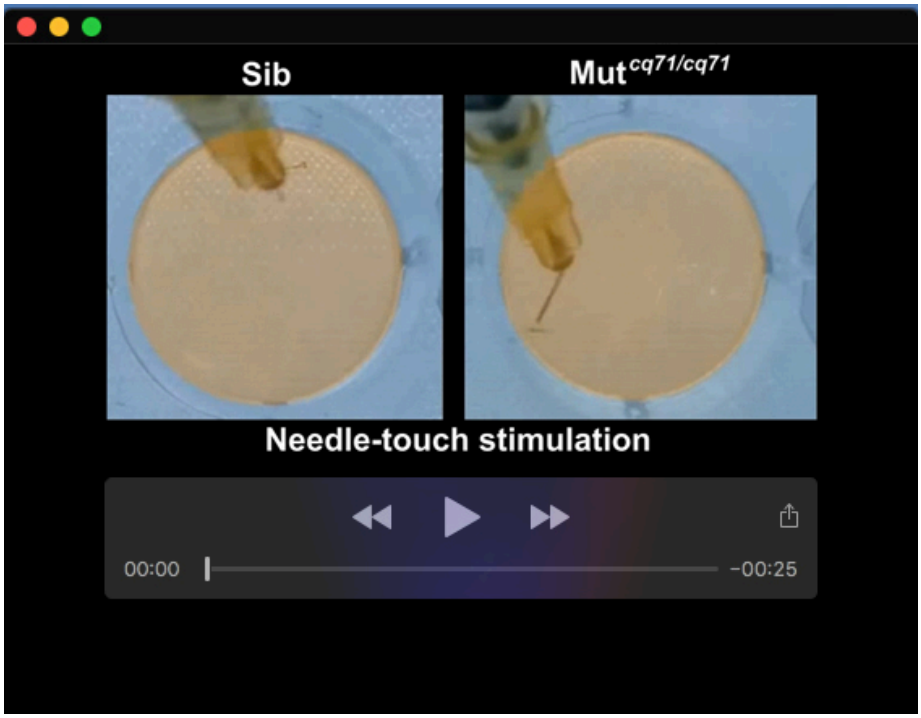

Movie 3. The sibling and Mut$^{cq71/cq71}$ mutant reactions on the needle-touch stimulation. Related to Figure S1. Three minutes track records of the swimming behaviors on 5 dpf larvae after a needle touch. The yellow circle area represents the imaging field. The red line represents the swimming track. This video presented the behavioral recording in Supplemental 1J.

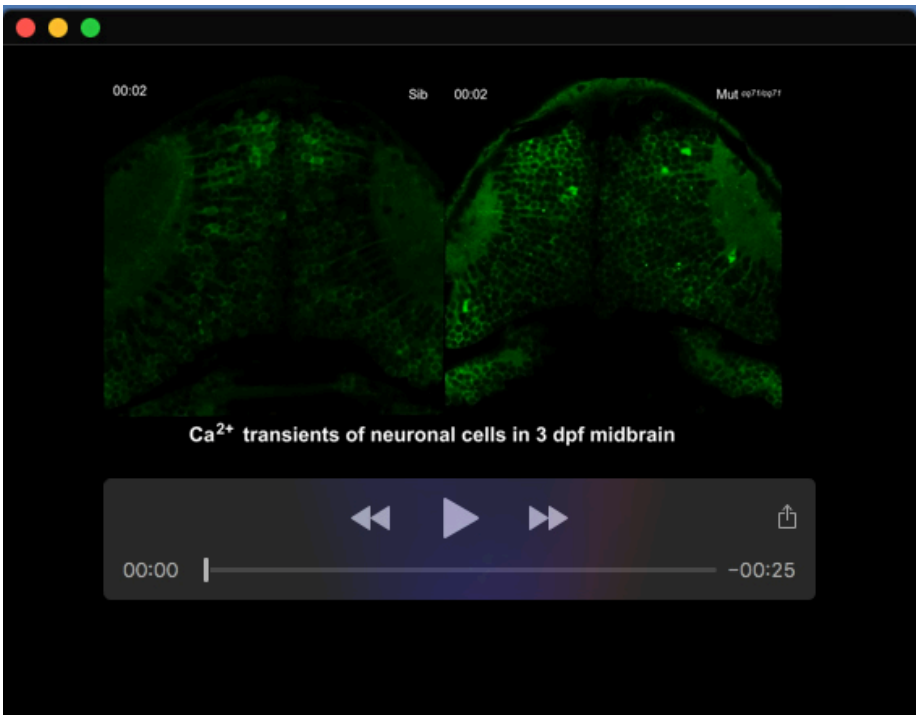

Movie 4. Spontaneous Ca^{2+} activity in the midbrains of sibling and Mut$^{cq71/cq71}$ mutant embryos. Related to Figure 1. Simultaneous calcium imaging of neuronal cells in 3dpf midbrains of *Tg(HuC:GCaMP6S)* embryos. Acquisitions were performed with scanning at 1.2 Hz at an excitation of 488 nm. The resolution was designed by 512 x 512 pixels on *Tg(HuC:GCaMP6s)*. And the time-length of single-layer imaging was 252 seconds in total, with 200 cycles. The selected fame images were given in Figure 1C.